

DEM-based river cross-section extraction and 1-D streamflow simulation for eco-hydrological modeling: a case study in upstream Hiikawa River, Japan

Tomohiro Tanaka¹, Hidekazu Yoshioka² and Yumi Yoshioka²

¹Graduate School of Global Environmental Studies, Kyoto University, Japan

²Graduate School of Natural Science and Technology, Shimane University, Japan

Abstract:

Simulating streamflow under both high- and low-flows is required for versatile eco-hydrological modeling. Typical streamflow simulators require hydrological data such as river geometry and observed river discharge/water level as upstream/downstream boundary conditions. However, these are not always available in data-sparse regions. Furthermore, because of the potential inaccuracy of digital elevation model (DEM) data around water surfaces, this data has not generally been utilized in streamflow simulations. Therefore, this study explores the potential applicability of DEM data to extract river cross-sections, focusing on the upstream Hiikawa River, Japan. A 1-D streamflow simulation was performed using river cross-sections extracted from a 5 m LiDAR DEM and the observed dam discharge from 2018 to 2020 as the upstream boundary condition. The simulated water depths with Manning's roughness coefficients of 0.03 to 0.05 m^{-1/3} s reproduce the observation results with Nash-Sutcliffe coefficients of 0.91–0.97 for the whole period and 0.60–0.97 for a flood event. The accurate results for both low and high flows were considered to reflect the reasonable representations of the river cross-section. Finally, the velocity-based suitability index for Ayu (*P. altivelis*) was evaluated. We demonstrate applicability and several possible limitations of DEM data for eco-hydrological modeling of data-scarce rivers.

KEYWORDS streamflow simulation; digital elevation models; river cross-section; Hiikawa river; eco-hydrology

INTRODUCTION

Streamflow simulations play a vital role in eco-hydraulic analysis of river environments. Conventional models to evaluate the habitat suitability of aquatic species such as fish and algae use hydraulic data such as water depth and flow velocity as key inputs (Febrina *et al.*, 2015; Heath *et al.*, 2015). Many studies have focused on upstream reaches where the input observation data for river flow models, such as discharge, water level and river cross-section data, are scarce. Data scarcity for meteorological/hydrological variables, including the river discharge and water level, has been a major issue in hydrology (e.g. the

Prediction of Ungauged Basins (PUB) initiative of the International Association of Hydrological Sciences proposed by Sivapalan (2003) and reviewed by Hrachowitz *et al.* (2013)). This has motivated the development of globally available climate/hydrological databases such as APHRODITE (Yatagai *et al.*, 2012) or the Global Runoff Data Center (GRDC) discharge datasets, data-assimilation techniques with hydrodynamic models, or globally available databases. In contrast, the scarcity of river geometry data has received less attention. Recently, high-resolution global terrain and hydrological datasets, mainly comprising flow directions and water body areas, have been developed (Yamazaki *et al.*, 2019; Lin *et al.*, 2021). However, the availability of river cross-section geometry data remains a significant issue. Only a few studies have applied widely available digital elevation data to the extraction of river cross-sections for streamflow modeling (Gichamo *et al.*, 2012; Zheng *et al.*, 2018).

The objective of this study is to demonstrate the potential of digital elevation model (DEM) based river cross-section extraction and its implementation in eco-hydrological modeling studies. This study targets the upstream Hiikawa River, Japan, where no measurements of the river cross-section are available. River cross-section data are created from LiDAR data at 5 m resolution provided by the Geospatial Information Authority of Japan (GIAJ). The 1-D local inertial equation (Bates *et al.*, 2010) is employed to simulate the streamflow in the river using the outflow discharge from an upstream dam (Obara Dam) as the inflow boundary condition. The simulated water depth is then compared with the observed water levels from 2019 to 2020. Finally, a brief new application of the streamflow simulation to evaluate the habitat suitability index for Ayu *Plecoglossus altivelis altivelis* (*P. altivelis*) is presented.

STUDY AREA

This study targeted the upstream reach of the Hiikawa River (Figure 1), which is a first-class river in the San-in area of Japan with a length of 153 km, a watershed area of 2070 km², and riverbed gradients of greater than 0.010, 0.00125 to 0.0050, and less than 0.001 in the upstream, middle-stream, and downstream reaches, respectively. The study area is located between the upstream and middle-

Correspondence to: Tomohiro Tanaka, Graduate School of Global Environmental Studies, Kyoto University, Kyotodaigaku-katsura, Nishikyo-ku, Kyoto 615-8540, Japan. E-mail: tanaka.tomohiro.7c@kyoto-u.ac.jp

Received 11 May, 2021

Accepted 22 June, 2021

Published online 18 August, 2021

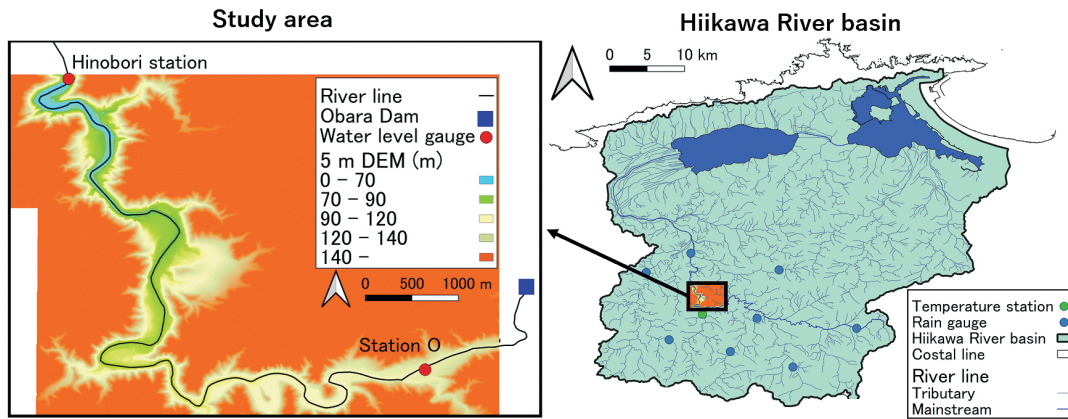


Figure 1. Map of the Hiikawa River basin and the study area. The blue and green circles in the basin map show the locations of rain gauges and the temperature station. A 1-D river flow simulation (and 2-D flood simulation if overflow occurs) was performed within the black frame (zoomed in view shown in the left panel) with elevation data. The water depth at Station O observed by the authors was used for validation

stream reaches. The watershed receives a total annual rainfall of 1900 mm (Ministry of Land, Infrastructure, Transportation and Tourism: MLIT, 2009). Obara Dam is a multi-purpose dam providing water resources and flood mitigation and is the largest dam constructed on the Hiikawa River; hourly operation data is available from April 2016. The downstream reaches of Obara Dam serve as a habitat for *P. altivelis*, the main inland fishery resource of the river. Their preferred range of water velocities was studied by Onitsuka *et al.* (2009). Recently, severe blooming of filamentous green algae on the riverbed has become an ecological issue because they exclude benthic diatoms and some cyanobacteria that serve as staple foods of *P. altivelis*. The filamentous green algae blooms have been suggested to be hydraulically controllable; in particular, there seems to be a threshold discharge at a relatively low flow above which the filamentous green algae are effectively removed from the riverbed (Yoshioka and Yaegashi, 2018). In contrast, predicting high flow discharges, such as floods caused by typhoon events, is also a critical issue. Both low and high flows are therefore of importance for analyzing the streamflow dynamics of the Hiikawa River.

DATA AND METHODS

DEM-based river cross-section extraction

Studies on streamflow simulations typically employ ground measurements of river cross-sections provided by the river management office for the target rivers or local unmanned aerial vehicle (UAV)-borne observations using drones (e.g. Lee *et al.*, 2019; Mazzoleni *et al.*, 2020). However, such data are usually unavailable in upstream reaches with no dike systems, as was the case in the target reach in this study.

As a more reasonable and widely available engineering alternative, this study employs the 5 m DEM provided by the GIAJ, which is available for most parts of Japan. River cross-section data were extracted by manually identifying the embankment locations of the river cross-section using Google Maps at intervals of approximately 200 m along the

reach (60 sites in total) and cutting out the elevations at 50 points along each cross-section. The direct use of DEM data without any bias correction for hydrological/hydrodynamic simulations is not preferred as it can introduce additional uncertainty, especially around the water surface area, where laser observations cannot capture the riverbed elevation accurately (Gichamo *et al.*, 2012; Zheng *et al.*, 2018). However, it may be reasonable to assume that the water depth during the LiDAR survey was sufficiently low compared to the total height from the riverbed to the embankment. In the Hiikawa River, the observed water depth is around 0.1 m excluding high-flow periods. In this context, we demonstrate that uncertainty in the laser observation around the riverbed has a small impact on the overall streamflow modeling.

The Hiikawa River Office has collected 1 m LiDAR DEM data. However, laser measurements on the water surface area (predefined as vector data) have been excluded from the database, possibly for some technical reasons (an example of the extracted cross-sections is shown in Figure S1: the 1 m LiDAR DEM is missing a larger area around the center, i.e. the water surface area, compared to the 5 m DEM from the GIAJ). If the missing data are interpolated from the nearest grids, the resulting 1-D streamflow simulation will be unstable owing to spuriously steep gradients (see the histogram of the riverbed gradients over the study area for both DEMs in Figure S2). Therefore, this study only used the 5 m DEM.

River flow modeling

This study applies the inundation model coupling rainfall-runoff components (IMCR) (Tanaka *et al.*, 2017) for the streamflow simulation. The IMCR simultaneously simulates the streamflow and surface runoff using 1-D and 2-D local inertial equations in the river and its floodplains, respectively. The semi-implicit scheme (Bates *et al.*, 2010) can stabilize the numerical simulation (Tanaka *et al.*, 2017). The IMCR can couple any distributed hydrological models to provide lateral inflows. This study employed a 1 km distributed hydrological model (1K-DHM) (Tanaka and Tachikawa, 2015) with surface and sub-surface kinematic

wave flow components as the hydrological model, as detailed in the next subsection.

The upstream boundary condition was provided by the actual hourly outflow discharge from the Obara Dam (Figure 1). The downstream boundary was located at the Hinobori Weir, with a height of 20 m, where there were publicly available water level observations. Both data were downloaded from Water Information System of the MLIT (<http://www1.river.go.jp/>). This study evaluated two different downstream boundary conditions: the observed water level, and a uniform flow condition, which assumes a more data-scarce situation. The target period for the streamflow simulation was from 2018 to 2020. The spatial resolution along the river was 50 m and the temporal resolution was first set as 0.5 s; the latter was adaptively updated at each time step based on the Courant-Friedrichs-Lewy condition with a safety factor of 0.7.

Rainfall-runoff modeling

A kinematic wave-based distributed hydrological model, 1K-DHM, was applied to model the rainfall-runoff processes in the upstream Hiikawa River basin, including the sub-basin for the study reach. The parameters for sub-surface modeling in the surface soil layers were calibrated based on the observed inflow hydrograph at the Obara Dam during a flood event in 2018 using the SCE-UA method (Duan *et al.*, 1994). Rainfall data were obtained from gauged observations collected by MLIT. An optimized hydrograph can effectively reproduce the observed hydrograph with a Nash-Sutcliffe coefficient of 0.92. Then, a rainfall-runoff simulation during the target period was performed using the calibrated 1K-DHM to simulate the lateral inflow to be provided to the IMCR. The evapotranspiration was estimated using the Thornthwaite method based on the monthly mean temperature.

Water depth observation for reference data

There are no observation data available between the Obara Dam and Hinobori gauging stations from the MLIT. The authors collected observed water depths from 2018 to 2020 near the former Onsen elementary school (hereinafter, Station O) (see Figure 1) using a pressure-type water gauge (CO-U20-001-04, HOBO; sampling error ± 0.3 cm) with a sampling interval of 10 min. However, there was a significant data deficit in the observations of 2018 due to machine failures. Therefore, we validated the model using the observed data from 2019 to 2020. Considering the uncertainty of the settlement location of the equipment and the height of the sensor from the riverbed, the observed water depth was corrected to +5 cm during the entire period.

RESULTS AND DISCUSSION

Simulation results from 2019 to 2020

The simulated and observed water depth hydrographs at Station O are shown in Figure 2. The observed depth in 2019 was stable at approximately 0.10 m, while in 2020, the water depth was more dynamic. A reason for the contrasting water depth changes is that the inflow to the Obara Dam was reduced by water withdrawal at an upstream hydropower plant until the end of May 2020, and since then

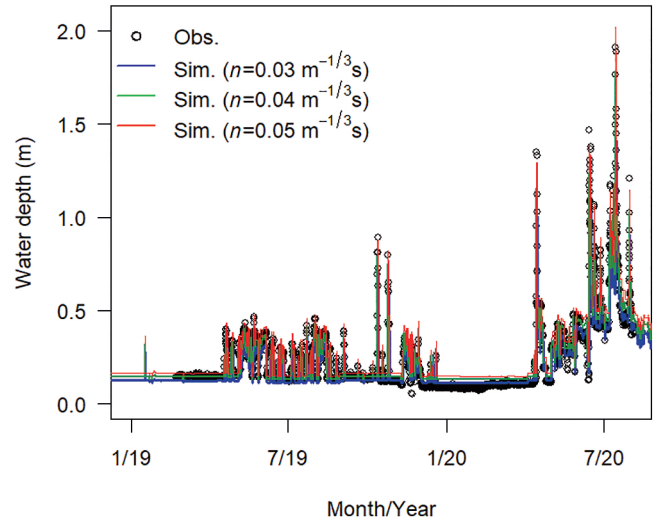


Figure 2. Time series of the simulated (lines) and observed (dots) water depths from 2019 to 2020 at Station O. The blue, green, and red lines show the simulation with Manning's roughness coefficients of 0.03, 0.04, and 0.05 $\text{m}^{-1/3} \text{s}$, respectively

the plant has been idling for repair. The relatively low rainfall of 1422 mm in 2019 compared with a typical rainfall of 1900 mm in normal years, may be another reason for the observed water depth changes. The Obara Dam releases $1.0 \text{ m}^3 \text{ s}^{-1}$ as a maintenance flow corresponding to a constant low water depth.

The simulated water depth accurately reproduced the dynamic changes in the observation data throughout the computational period. The simulation results with different Manning's coefficients (0.03 to 0.05 $\text{m}^{-1/3} \text{ s}$) show a comparably accurate performance, with Nash-Sutcliffe efficiency (NSE) values ranging from 0.91 to 0.97 for the whole period. As an example of high flows, a flood event during July 13–14, 2020 is shown in Figure 3, demonstrating the high accuracy of the simulated result, with NSE values of 0.60 to 0.97 (additional details are given in Table I).

Impact of site-specific observation data

The impacts of the absence of an observed water level at the Hinobori station for use as the downstream boundary condition were examined by specifying a common uniform flow condition at this boundary. Figure 4 shows an example of the water surface profile from the Hinobori station to 3 km upstream (the entire study reach is approximately 15 km) at 0:00 on July 14, 2020 with and without the observed water level data. The study reach is so steep that the impacts of the boundary conditions are negligible in the reaches more than 1 to 2 km upstream. Accordingly, no difference was found between the two cases at the reference station 14 km upstream (see Figure S3).

This study directly used the outflow discharge at the Obara Dam. In addition, the target reach receives a marginal impact of lateral inflow to the volume (approximately 0.3% of the outflow discharge at the Obara Dam). Therefore, the absence of river cross-section data is considered the largest obstacle to simulating the water level in the

Table I. Performance indices (Nash-Sutcliffe efficiency (NSE) and Root mean square error (RMSE)) for the whole simulation period and a flood event with different Manning’s roughness coefficients (n)

	Whole period			Flood event in July 2020		
n ($\text{m}^{-1/3} \text{s}$)	0.03	0.04	0.05	0.03	0.04	0.05
NSE	0.95	0.97	0.91	0.60	0.91	0.97
RMSE	0.054	0.033	0.042	0.264	0.125	0.070

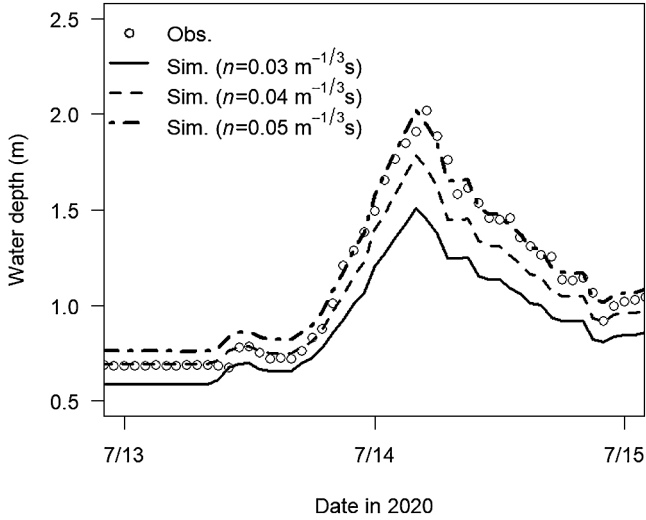


Figure 3. Time series of simulated (lines) and observed (white circles) water depths at Station O for the flood event of July 13–15, 2020

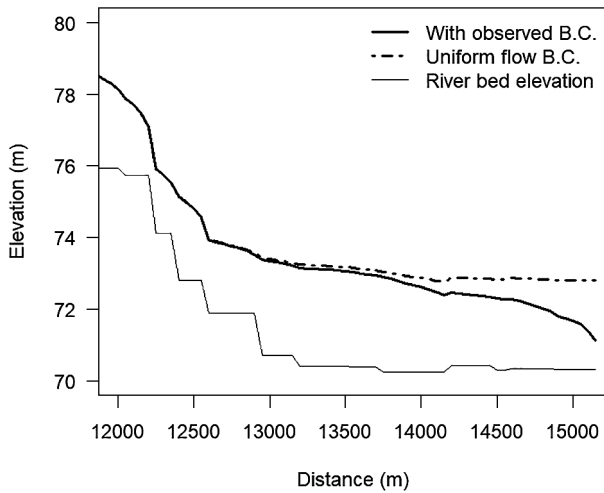


Figure 4. Longitudinal plot of the simulated water level near the downstream boundary (12 to 15 km from the upstream boundary) with and without the observed downstream boundary condition (B. C.) of water level (shown with solid and dashed lines, respectively). The thin solid line shows the riverbed elevation extracted from the 5 m DEM

study region; this obstacle was successfully overcome by the DEM-based river cross-section extraction. However, in

general, the simulation accuracy is also a source of uncertainty, and thus it should be systematically investigated to achieve reliable simulation results (Butts *et al.*, 2004).

Impact of DEM quality

As discussed above, the high reproducibility of the simulated water depth depends on the quality of 5 m DEM that we used for preparing the river cross-section data. In more general cases, the quality could be degraded due to 1) coarse spatial resolution of available DEM and 2) LiDAR measurements during higher water level. Their impacts were explored by 1) upscaling 5 m DEM to 10 m and 32 m (averaging for two and six cells, respectively) and 2) limiting the DEM above 30 cm, 50 cm, and 100 cm of the bottom elevation (corresponding to 40%, 10% and 1% of hourly depth quantiles, respectively). For example, limiting the DEM above 30 cm reflects the situation where the true water surface exists 30 cm above the bottom elevation during the LiDAR measurements. Both resulted in underestimation of the water depth especially when the DEM was upscaled to 32 m (Figure S4) and cut by 50 cm (Figure S5). This is because smoothing elevation profiles or employing cross-section at higher water level leads to wider river widths. These findings suggest that the accurate 1-D river flow simulation with the DEM-based cross-section extraction in this study is owing to the high spatial resolutions of DEM (< 10 m) and LiDAR measurements at low flow conditions (< 30 cm).

Suitability index (SI) simulation using the flow velocity preference curve for Ayu

Finally, we present an example of a simple new application of the streamflow simulation. The application here is not intended as a complete analysis of the suitability index, but rather a preliminary report of a new computational result. The study reach is a habitat of *P. altivelis* from May to October/November, and harvesting the fish is allowed between July and October. The habitat suitability of the study reach for these fish has been a serious concern because the species is the main fishery resource in this river. However, the habitat suitability of *P. altivelis* has not yet been analyzed in this river.

Onitsuka *et al.* (2009) proposed the following gamma distribution model to estimate the preference curve relating the flow velocity and suitability index (SI) for *P. altivelis* $SI(v)$:

$$SI(v) = \frac{1}{\Gamma(\lambda)} \alpha^\lambda v^{\lambda-1} e^{-\alpha v} \quad (1)$$

where v is the flow velocity (m s^{-1}), Γ is the Gamma function, and α and λ are model parameters, which are 1.50 and 1.25, respectively, in this study according to the literature.

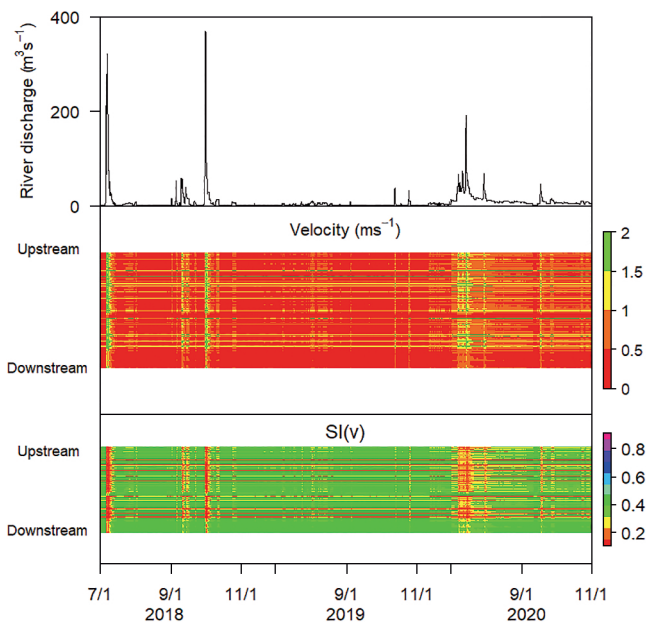


Figure 5. Time series of the simulated river discharge (top) at Station O (see Figure 1), flow velocity (middle) and suitability index (SI) (bottom) over the study reach during July to November in 2018 to 2020

The estimated SI from July to November in 2018 to 2020, during which *P. altivelis* remain in the target reach, is plotted in the bottom panel of Figure 5. The river discharge and flow velocity at Station O are also shown in the upper and middle panels, respectively. Obviously, the flow velocity is higher during high-flow periods, during which the SI is smaller over the reach. There are hotspots where the cross-section is locally narrow, at which the flow velocity becomes locally high, and the local SI becomes lower (typically 2.0 to 7.0 km from the upstream boundary) than in other parts of the target reach. The cumulative suitability index (CSI), which includes other components such as the water depth, riverbed properties, and flow velocity will be addressed in future research. Our application here focused on a longitudinal simulation but not a horizontal 2-D simulation; further, other hydrological indexes such as water temperature and water quality should also be considered for a more sophisticated analysis of habitat suitability. For example, fish including *P. altivelis* seek refuge areas where the local flow velocity is not too high. This will be the next step. Nevertheless, our application provides preliminary spatiotemporal information about the suitability index of *P. altivelis* in the target reach.

CONCLUDING REMARKS

We proposed a DEM-based engineering method and easily implementable approach for dealing with stream flows, including both high and low discharges, in the eco-hydrological modeling of upstream river reaches. We explored the direct use of widely available 5 m DEM data for the upstream Hiikawa River as a case study.

Owing to the available outflow discharge data from the

Obara Dam, the accuracy of the 1-D streamflow simulation mostly depended on the representation of the river geometry. As a result, the 1-D river flow simulation with local inertial equations using the DEM-based extracted river cross-section demonstrated highly versatile performance. The study area had a small impact on the downstream water level because of the steep gradient in the target reach, which is a common feature of mountainous rivers. The sensitivity analysis of DEM quality suggested that the high performance was owing to the high resolution and coverage (low flow conditions) of the LiDAR measurements. Finally, a preliminary application of the simulated flow velocity to estimate the SI for a fish species was demonstrated. This case study demonstrated the high potential of using widely available DEM data for river cross-section extraction and river flow simulation in eco-hydrological modeling in mountainous areas. In particular, the analysis supports future predictions of streamflow dynamics in the target reach corresponding to hypothetical outflow discharge scenarios from the Obara Dam. This is an important topic to be addressed in future studies.

ACKNOWLEDGMENTS

The Grant for Environmental Research Projects from the Sumitomo Foundation 203160 supported this research. The 1 m LiDAR DEM was provided by the Hiikawa River Office. Mr. Masafumi Kato, a master course student at the Hydrology and Water Resources Laboratory, Kyoto University, helped apply the 1K-DHM to the upstream Hiikawa River basin and identify river bank locations.

SUPPLEMENTS

Figure S1. Example of the river cross-sections obtained using the 5 m DEM provided by the Geospatial Information Authority of Japan that is available for most areas in Japan and the 1 m DEM provided by the Hiikawa River Office for the study area. The 1 m DEM is missing elevation data for the predefined water surface area (around 40 to 90 m from the left bank).

Figure S2. Histogram of the riverbed gradients for river cross-sections extracted from the 5 m DEM provided by the Geospatial Information Authority of Japan that is available for most areas in Japan and the 1 m DEM provided by the Hiikawa River Office for the study area. Owing to missing elevation data for the water surface areas, the 1 m DEM leads to artificially steep slopes, increasing the instability of the river flow simulation.

Figure S3. Time series of the observed water depth (dots) and simulated water depth at Station O (see Figure 1) from 2019 to 2020 with (blue solid line) and without (black broken line) the observed water level boundary condition (B. C.)

Figure S4. Time series of the simulated water depth at Station O (see Figure 1) from 2019 to 2020 with the original (black) DEM and the DEM resolution upscaled to 10 m (red) and 32 m (green). The Manning roughness coefficient n was set at $0.05 \text{ m}^{-1/3} \text{ s}$

Figure S5. Time series of the simulated water depth at Sta-

tion O (see Figure 1) from 2019 to 2020 with the original (black) DEM and the DEM only above 30 cm (blue), 50 cm (green) and 100 cm (red) given that the true water surface exists above the bottom elevation during the LiDAR measurements. The Manning roughness coefficient n was set at $0.05 \text{ m}^{-1/3} \text{ s}$

REFERENCES

- Bates PD, Horritt MS, Fewtrell TJ. 2010. A simple inertial formulation of the shallow water equations for efficient two-dimensional flood inundation modelling. *Journal of Hydrology* **387**: 33–45. DOI: 10.1016/j.jhydrol.2010.03.027.
- Butts MB, Payne JT, Kristensen M, Madsen H. 2004. An evaluation of the impact of model structure on hydrological modelling uncertainty for streamflow simulation. *Journal of Hydrology* **298**: 242–266. DOI: 10.1016/j.jhydrol.2004.03.042.
- Duan Q, Sorooshian S, Gupta VK. 1994. Optimal use of the SCE-UA global optimization method for calibrating watershed models. *Journal of Hydrology* **158**: 265–284. DOI: 10.1016/0022-1694(94)90057-4.
- Febrina R, Sekine M, Noguchi H, Yamamoto K, Kanno A, Higuchi T, Imai T. 2015. Modeling the preference of ayu (*Plecoglossus altivelis*) for underwater sounds to determine the migration path in a river. *Ecological Modelling* **299**: 102–113. DOI: 10.1016/j.ecolmodel.2014.12.010.
- Gichamo TZ, Popescu I, Jonoski A, Solomatine D. 2012. River cross-section extraction from the ASTER global DEM for flood modeling. *Environmental Modelling & Software* **31**: 37–46. DOI: 10.1016/j.envsoft.2011.12.003.
- Heath MW, Wood SA, Brasell KA, Young RG, Ryan KG. 2015. Development of habitat suitability criteria and in-stream habitat assessment for the benthic cyanobacteria *Phormidium*. *River Research and Applications* **31**: 98–108. DOI: 10.1002/rra.2722.
- Hrachowitz M, Savenije HHG, Blöschl G, McDonnell JJ, Sivapalan M, Pomeroy JW, Arheimer B, Blume T, Clark MP, Ehret U, Fenicia F, Freer JE, Gelfan A, Gupta HV, Hughes DA, Hut RW, Montanari A, Pande S, Tetzlaff D, Troch PA, Uhlenbrook S, Wagener T, Winsemius HC, Woods RA, Zehe E, Cudennec C. 2013. A decade of Predictions in Ungauged Basins (PUB) – a review. *Hydrological Sciences Journal* **58**: 1198–1255. DOI: 10.1080/02626667.2013.803183.
- Lee G, Choi M, Yu W, Jung K. 2019. Creation of river terrain data using region growing method based on point cloud data from UAV photography. *Quaternary International* **519**: 255–262. DOI: 10.1016/j.quaint.2019.04.005.
- Lin P, Pan M, Wood EF, Yamazaki D, Allen GH. 2021. A new vector-based global river network dataset accounting for variable drainage density. *Scientific Data* **8**: 1–9. DOI: 10.1038/s41597-021-00819-9.
- Mazzoleni M, Paron P, Reali A, Juizo D, Manane J, Brandimarte L. 2020. Testing UAV-derived topography for hydraulic modelling in a tropical environment. *Natural Hazards* **103**: 139–163. DOI: 10.1007/s11069-020-03963-4.
- Ministry of Land, Infrastructure, Transportation and Tourism. 2009. Overview of the Hiikawa River basin. https://www.mlit.go.jp/river/basic_info/jigyo_keikaku/gaiyou/seibi/pdf/hiikawa72-5-1.pdf. Last access April 27, 2021.
- Onitsuka K, Nagaya T, Shiraiishi Y, Ukese A, Higashino M, Takami T, Yokomine S, Akiyama J, Ono A, Serikawa T. 2009. A proposal of preference curves of velocity for Ayu. *Environmental Engineering Research* **46**: 29–38.
- Sivapalan M. 2003. Prediction in ungauged basins: a grand challenge for theoretical hydrology. *Hydrological Processes* **17**: 3163–3170. DOI: 10.1002/hyp.5155.
- Tanaka T, Tachikawa Y. 2015. Testing the applicability of a kinematic wave-based distributed hydrological model in two climatically contrasting catchments. *Hydrological Sciences Journal* **60**: 1361–1373. DOI: 10.1080/02626667.2014.967693.
- Tanaka T, Tachikawa Y, Ichikawa Y, Yorozu K. 2017. Impact assessment of upstream flooding on extreme flood frequency analysis by incorporating a flood-inundation model for flood risk assessment. *Journal of Hydrology* **554**: 370–382. DOI: 10.1016/j.jhydrol.2017.09.012.
- Yamazaki D, Ikeshima D, Sosa J, Bates PD, Allen GH, Pavelsky TM. 2019. MERIT Hydro: A high-resolution global hydrography map based on latest topography dataset. *Water Resources Research* **55**: 5053–5073. DOI: 10.1029/2019WR024873.
- Yatagai A, Kamiguchi K, Arakawa O, Hamada A, Yasutomi N, Kitoh A. 2012. APHRODITE: Constructing a long-term daily gridded precipitation dataset for Asia based on a dense network of rain gauges. *Bulletin of the American Meteorological Society* **93**: 1401–1415. DOI: 10.1175/BAMS-D-11-00122.1.
- Yoshioka H, Yaegashi Y. 2018. Robust stochastic control modeling of dam discharge to suppress overgrowth of downstream harmful algae. *Applied Stochastic Models in Business and Industry* **34**: 338–354. DOI: 10.1002/asmb.2301.
- Zheng X, Tarboton DG, Maidment DR, Liu YY, Passalacqua P. 2018. River channel geometry and rating curve estimation using height above the nearest drainage. *Journal of the American Water Resources Association* **54**: 785–806. DOI: 10.1111/1752-1688.12661.